Citation: Firas F. Qader, Falah Z. Mohammed, Barhm Mohamad. Thermodynamic analysis and optimization of flat plate solar collector using TiO_2/water nanofluid. *Journal of Harbin Institute of Technology (New Series)*. DOI: 10.11916/j.issn.1005-9113.2023050

Thermodynamic Analysis and Optimization of Flat Plate Solar Collector Using TiO_2 /Water Nanofluid

Firas F. Qader[1], Falah Z. Mohammed[2] and Barhm Mohamad[3]*

(*1. Technical Engineering College-Kirkuk, Northern Technical University, Kirkuk 36001, Iraq;*
2. Medical Device Technology Engineering, AL-Qalam University College, Kirkuk 36001, Iraq;
3.Department of Petroleum Technology, Koya Technical Institute, Erbil Polytechnic University, Erbil 44001, Iraq)

Abstract: To research solar energy's efficiency and environmental benefits, the thermal efficiency, exergy, and entropy of solar collectors were calculated. The experiment involved two glass-topped collectors, fluid transfer tubes, and aluminum heat-absorbing plates. Glass wool insulation minimized heat loss. A 0.5% TiO_2/Water nanofluid was created using a mechanical and ultrasonic stirrer. Results showed that solar radiation increased thermal efficiency until midday, reaching 48.48% for water and 51.23% for the nanofluid. With increasing mass flow rates from 0.0045 kg/s to 0.02 kg/s, thermal efficiency improved from 16.26% to 47.37% for water and from 20.65% to 48.76% for the nanofluid. Filtered water provided 380 W and 395 W of energy in March and April, while the nanofluid increased it to 395 W and 415 W during these months. Mass flow generated energy, and the Reynolds number raised entropy. The noon exergy efficiency for nanofluids was 50%-55%, compared to 30% for water. At noon, the broken exergy measured 877.53 W for the nanofluid and 880.12 W for water. In Kirkuk, Iraq, the 0.5% TiO_2/Water nanofluid outperformed water in solar collectors.

Keywords: energy; exergy; entropy generation; nanofluid; flat plate solar collector
CLC number: TK51 **Document code**: A **Article ID**: 1005-9113(2023)00-0000-14

0 Introduction

This study focused on improving the performance of a flat solar collector by using nanofluid. In recent literature, the researchers used a MWCNT-H_2 O nanofluid with a diameter of 10-30 nm and a weight concentration of 0.2% - 0.4% to increase the collector's efficiency by 83%. In this study, the thermal efficiency of the collector is linearly related to nanoparticle mass flow rate and volumetric concentration. By using a nano-diamond fluid with a concentration of 1% and a percentage of 69.8% compared to water, the flat solar collector's efficiency was maximized. The study also measured the viscosity of the nanofluid and water using the Brookfield Digital Viscometer DV-II + Pro. The experiments were conducted for two months in Kirkuk's climate, and the margin of error was found. Overall, the results suggest that using nanofluid can significantly improve the efficiency of flat solar collectors. To improve the performance of a 2-square-meter-squared flat solar collector, Yousefi and Veisy[1] used a MWCNT- m^2 nanofluid with a diameter of 10-30 nm, a weight concentration of 0.2%-0.4%, and a mass flow rate of 0.0167-0.05 kg/s. The flat solar collector's efficiency rose 83% by increasing mass flow rate and nanofluid concentration. An experimental research was carried out on a 0.34 m^2 flat solar collector using CNT nanofluid with a diameter of 1 nm and weight concentrations of 0.6%, 0.5%, and 0.4%[2]. At 0.5%, efficiency increased by 39%. An experimental evaluation of thermal performance in a flat solar collector of 1 m^2 area, Zamzamian et al.[3] employed Cu nanofluids combined with ethanol alcohol with a diameter of 10 nm, volumetric concentrations of

Received 2023-05-10.
Corresponding author. Barhm Mohamad, Ph.D., Lecturer. E-mail: barhm.mohamad@epu.edu.iq

0.2%-0.3% , and mass flow rates of 0.016 - 0.050 kg/s on a flat solar collector with a 0.67 m^2 surface and discovered that a concentration of 0.3%. Nasrin and Alim[4] evaluated the thermal performance of a 1.51 m^2 solar collector. In distilled water, 50 nm Al_2O_3, 50 nm CuO, and 25 nm TiO_2 nanoparticles were used. Laminar flow was created using three nanoparticle concentrations (0.2%, 0.4%, and 0.8%) with a mass flow rate of 4.0 kg/min. The augmentation of surface heat transfer rate was observed with elevated nanoparticle concentration within the base liquid, dependent on the type of particles used. Notably, the presence of copper particles resulted in a significantly higher heat transfer rate compared to systems utilizing aluminum oxide and titanium oxide particles. The most notable enhancement, reaching 87.8%, was attained with copper oxide when employed alongside pure water, surpassing the improvement achieved using distilled water, which measured 52.5%. Moghadam et al.[5] performed an experimental investigation of the thermal performance of a 1.88 m^2 solar collector. With a mass flow velocity of kg/min and a diameter of 40 nm, CuO nanofluid with a mass concentration of 0.4% flows laminarly. The efficiency percentage was found to be 21.8% higher than when using water as the base fluid. Michael and Iniyan[6] saw that a CuO nanofluid with a diameter of 0.3, 0.4 nm mixed with water as the base and a volumetric concentration of 0.05% enhanced the thermal efficiency of a 2.184 m^2 solar collector. At 0.1 kg/min, the solar collector's efficiency is 57.98% compared to a forced load. Al_2O_3 nanofluid was mixed with distilled water with a diameter of 15 nm and volumetric concentrations varying from 0.090696% to 0.1423% and evaluated on a 1.51 m^2 flat solar collector. Adjusting parameters and lowering energy generally improves nanofluid efficiency when paired with water. Said et al.[7] evaluated a flat solar collector with an area of 1.84 m^2 using a 21 nm TiO_2 nanofluid at volumetric concentrations of 0.1% and 0.3%. Laminar flow produced 0.5 kg/min. The results showed a 76.6% efficiency improvement over water. Polyethylene Clay Cool PEG stabilized liquid. In an experimental study , on a flat solar collector with an area of 1.59 m^2, employed nanofluid TiO_2/EG-water with a diameter of 10 nm and volumetric concentrations to improve solar collector performance (0.5, 0.75, and 1). Turbulent flow was 2.7 kg/min. Efficiency increased 4-8 percentage points compared to water. Salavati Meibodi et al.[8] studied a flat solar collector with an area of m^2 using nanofluid TiO_2 with a diameter of 10 nm and volumetric concentrations to improve solar collector efficiency (0.2, 0.4 and 0.6). Turbulent flow was 3 kg/min. Compared to water; efficiency rose 23.5%. Vakili et al.[9] demonstrates that increasing the weight fraction of the nanofluid enhances collector efficiency, with the highest efficiency observed at a flow rate of 0.015 kg/s for both the base fluid and nanofluids, achieving zero-loss efficiencies of 83.5%, 89.7%, and 93.2% for weight fractions of 0.0005, 0.001, and 0.005, respectively, compared to 70% for the base fluid. Verma et al.[10] studied a flat solar collector with an area of 0.375 m^2 to find how MgO nanofluid with a diameter of 40 nm and varying volume concentrations 0.25%, 0.5%, 0.75%, 1.0%, 1.25% and 1.5% at 0.5, 1.0, 1.5, 2.0, 2.5 L/min respectively. At a concentration of 0.75% and a volumetric flow of 1.5 L/min, the collector's heat efficiency rose by 9.34% and its exergy efficiency by 32.2% compared to water. At 0.75% volumetric concentration, the entropy generated is 0.0611 W/k; at 1.5%, it is 0.1394 W/k and 0.071 W/k, respectively. Jouybari et al.[11] examined many techniques to boost the efficiency of 0.375 m^2 flat solar collectors, MWCNTS, graphene, CuO, SiO_2, TiO_2, and Al_2O_3 were nanoparticles. In water, 7 to 20 to 42 to 10 to 44 to 45 nm and 20% to 18% to 30% to 35% to 23% by weight. Researchers had seen those mixes of (TiO_2-m^2), (TiO_2-m^2), (Al_2O_3-m^2), (CuO - m^2), (Graphene - m^2), and (MWCNTS-m^2) had better ratios (5.74, 6.97, 10.86, 16.67, 21.46, 29.32) than water under liquid circumstances. Compared with water as the base fluid and the solar collector´s best energy efficiency, TiO_2-m^2, TiO_2-m^2, Al_2O_3-m^2, CuO-m^2 Graphene-m^2, and MWCNTS - m^2 lowered entropy by 10.04%, 24.49%, 36.84%, 48.32%, 57.89%, and 65.55%. A 0.8 m^2 solar collector was examined for thermal efficiency. Increasing solar collector efficiency by mixing water with a TiO_2 nanofluid with a diameter of 7 nm. Laminar flow was created using three nanoparticle concentrations (0.2%, 0.4%, and 0.8%) with a flow velocity of 1.5 kg/min. As proved experimentally, nanoparticle concentration in the base liquid promotes heat transmission, and particle type changes the flat surface collector. Efficiency rises by 8% over water. Syam Sundar et al.[12] and Zarda et

al.[13] tested Al_2O_3 nanofluids with diameters of 20 nm, concentrations of 0.1% and 0.3% by volume, and a flow rate of 5 kg/s on a 2 m^2 flat solar collector to increase efficiency. Compared to water, efficiency was 18% greater. Kiliç et al.[14] investigated a TiO_2 Triton X-100 nanofluid, characterized by a particle diameter of 44 nm and a volumetric concentration of 0.2%. This investigation employed a flat solar collector featuring a surface area of 1.82 m^2. The measurements were taken in seconds and pertained to mass-related quantities. Sharafeldin and Gróf[15] conducted a study investigating the impact of varying concentrations of CeO_2 nanofluid within water (used as the base fluid). The study focused on a flat solar collector with a surface area of 2.03 m^2, and the experiments were carried out at mass flow rates of 0.00167%, 0.0333%, and 0.0666%. The working fluid mass flux rates were measured at 0.019, 0.018, and 0.015 kg/s·m^2, the results of their research indicated that the utilization of a nanofluid instead of regular water as the base fluid led to a notable enhancement in collector efficiency. Specifically, the researchers observed a linear correlation between the collector's thermal efficiency and both the nanoparticle mass flow rate and the volumetric concentration of the nanofluid. Tong et al.[16] evaluated different concentrations of nanofluids (CuO, Al_2O_3) in water as the base fluid, with a diameter of 20-40 nm, on a flat solar collector with an area of 2 m^2 and 1.5 vol%-Al_2O_3 nanofluids instead of water raised flat solar collector efficiency to 21.9%. Water generated the most entropy, followed by 0.1% Al_2O_3 nanofluid. An Al_2O_3 nanofluid with a volumetric content of 0.1% and a CuO nanofluid with 0.5% boosted energy by 56% and 49.6%, respectively, compared to water. The flat solar collector's greatest thermal efficiency was achieved using 0.1% Al_2O_3 nanofluid in water. Nirmala[17] tested ways to improve flat solar collectors. In the sunlight, the distance between the glass and the absorbing plate was 2 cm, and at the same time and the same size as the flat solar collector, put the double glass plate at the same distance with the absorption plate, and the study found that the double glass plate doubles the efficiency of the flat solar collector compared to the single glass plate. Choudhary et al.[18] tested a 2.1 m^2 flat solar collector using nanofluid (ZnO) added to ethylene clay powder and distilled water with a 50 nm diameter. At 150 L/h, the collector's exit temperature is 318.62 K, and the flat solar collector's thermal efficiency increases from 30 to 150 L/h. At 60 L/h and 1% nanofluid concentration, thermal efficiency is 69.24%, 19.24% higher than with distilled water. Okonkwo et al.[19] examined single and hybrid nanofluids (Al_2O_3) and (Al_2O_3-Fe) using water as the base fluid using a flat solar collector of 1.51 m^2. The hybrid nanofluid lowered flat solar collector thermal efficiency by 1.79 percentage points compared to water, while nanofluid (Al_2O_3) at 0.1% enhanced thermal efficiency by 2.16 percentage points. Hybrid nanofluids boost exergy efficiency by 6.9% over solo nanofluids. Alklaibi et al.[20] conducted an experimental study on a flat solar collector to improve efficiency and heat transfer in an area of m^2 using nanofluid diamond mixed with water as the base fluid and concentrations of (0.2, 0.4, 0.6), 1.0%, and 0.8% and a mass flow of 0.02 kg/s. The flat solar collector's efficiency was maximized by using a nano-diamond fluid with a concentration of 1% and a percentage of 69.8% compared to water. We created entropy with a maximum of 5.725% and a minimum of 5.5415% using nanofluid.

1 Methodology

1.1 Experimental Configuration

After the planar solar collector's design, identification, and planning stages, each component's production techniques were developed, as shown in Fig.1.

The system's core is a 1 m^2 metal box. The shell has three plastic panels, an aluminum skin, and five centimeters of glass fiber between them. Clean glass covers it. The device is fixed and immovable with a 4 mm thickness to suit its large cross-sectional area, protect it from breakage and weather, and maximize energy absorbed from the top by allowing solar radiation to penetrate and reducing thermal losses from the front side of the complex and from the bottom and sides. Insulated from heat. Electrically mixing TiO_2 and water formed a nanofluid for the second part. Ensure water nanoparticle dispersion. Copper tubes measuring 0.85 m long make up the solar collector:

The header tubes' inner diameter is 22.5 mm, and their thickness is 1 mm. The riser tube's inner diameter is 9.5 mm, and its thickness is 1.5 mm. Pipes linking system components were insulated with two layers of Armaflex insulation to prevent heat loss through the tank walls. German-made 21-inch plastic tubes connected the solar collectors and tanks, plastic tubes

couplings, and valves-controlled water and nanofluid flow. Two quarter-horsepower vertical pumps at least 2.5 m tall, moved water and nanofluid through the system as shown in Fig.2.

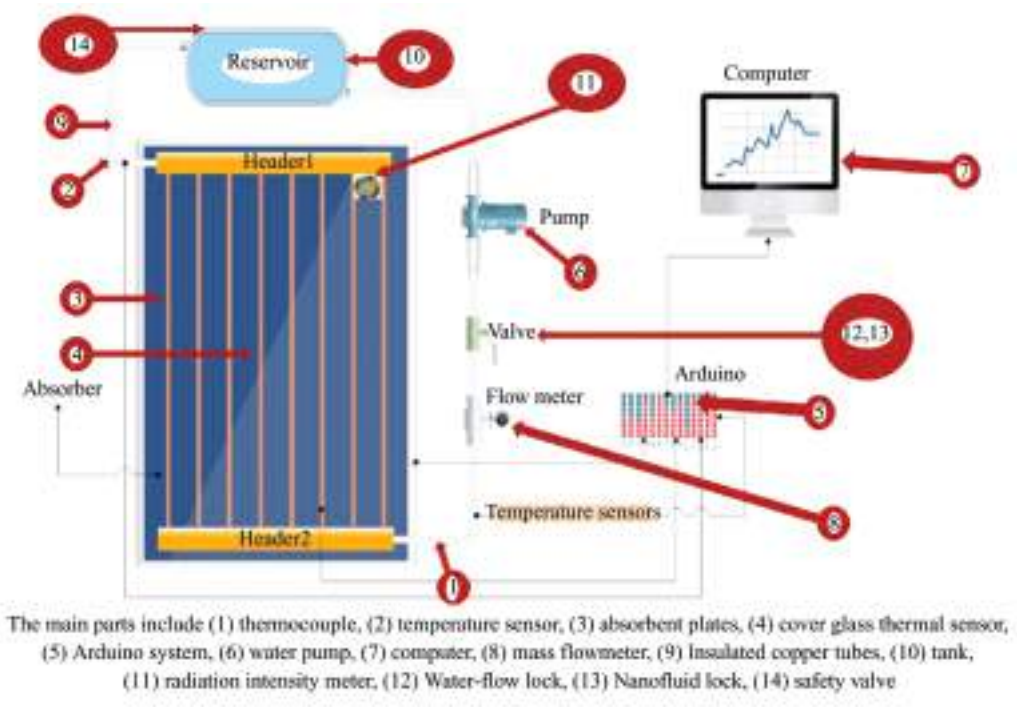

Fig.1 Scheme of planar solar collector

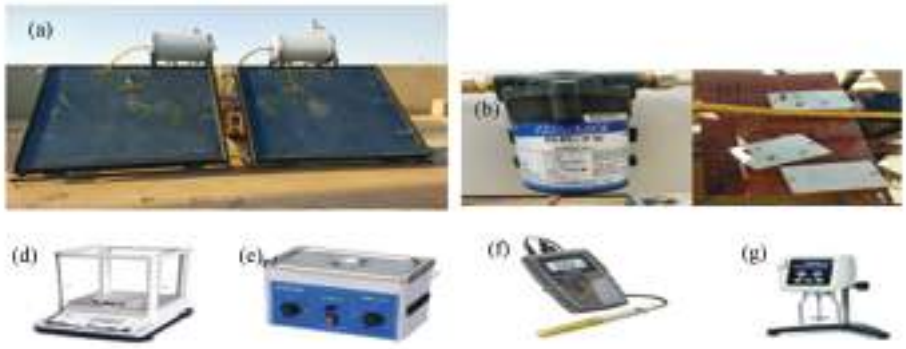

Fig.2 The experiment apparatus includes (a) Solar collectors, (b) fluid pump, (c) Arduino system, (d) sensitive scale, (e) Ultrasound nano equipment, (f) indicator of thermal conductivity, (g) images depicting the process of measuring viscosity

The nanofluid test device pushes nanofluid and pure water to a flat solar collector from their tanks and detect water and nanofluid velocities. Two iron bases held the fluid tank, the flat solar collector for the water and nanofluid systems, two flow meters, and digital temperature scales to create the test system. The main parts are listed in Table 1.

1.2 Instruments for Sensing Temperature and Associated Math for Calibration

The electrical circuit's most crucial component, the Arduino chip, recorded fluid temperatures at the primary and secondary flat solar collectors' entrances and exits and radiation intensity flow rate. A memory card retained Arduino data permanently. The study's variables fit the Arduino UNO's 12 connection points. Each system (pure water and nanofluid) is pre-programmed to record seven data points per hour: entrance temperature, exit temperature, absorption plate temperature, glass cover temperature, ambient temperature, flow rate amount, and radiation intensity. Fig.2(c) shows data from four digital and four analog heat sensors coupled to Arduino systems (K and NTC).

A mercury thermometer and a Celsius-graded mercury thermometer are used to calibrate thermocouple

sensors (0-100). Fig.3 shows the mercury thermometer and temperature sensors calibrated for a flat solar collector. They record temperatures until they boil at 100 ℃ in a glass container with frozen water at 0 ℃.

Table 1 Main parts of the test system

No.	System parts	No.	System parts
1	Water entry temperature sensor (thermocouple) for solar collectors (pure water system and nanofluid system)	8	Both system mass flowmeter
2	Water outflow temperature sensor (thermocouple) for solar collectors (pure water system and nanofluid system)	9	Insulated copper tubes
3	Thermal sensor for two systems´ absorbent plates (water and nanofluid)	10	Two tanks that can hold clean water and nanofluid (45 L)
4	Two-system cover glass thermal sensor (water and nanofluid)	11	Two radiation intensity meters for each system
5	Two Arduino system keys for pure water and nanofluid	12	Water-flow lock
6	The nanofluid and pure water pump switch	13	Nanofluid lock
7	Computer to read data.	14	Dual tank safety valve (pure water and nanofluid).

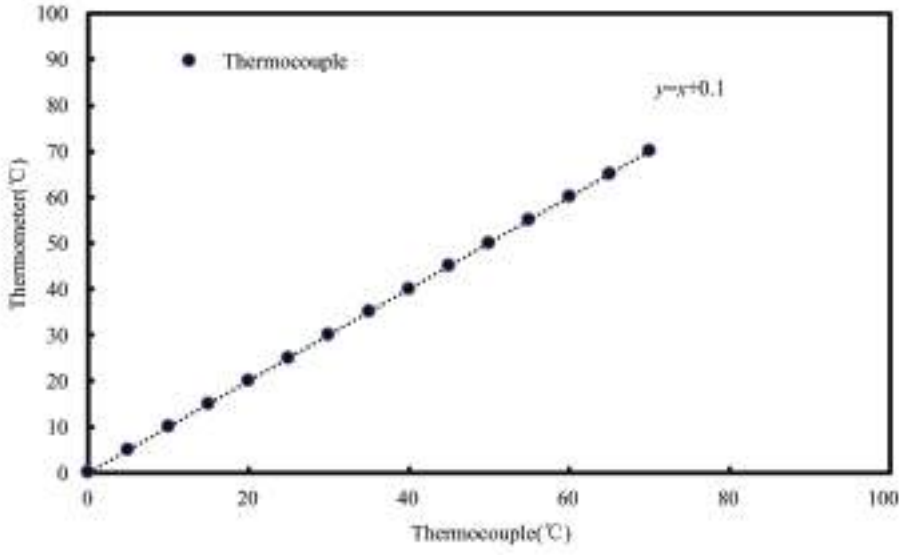

Fig.3 Temperature sensor calibration

2 Preparation of Nanofluids

Nanofluid preparation begins with finding the volumetric ratio, or particle concentration in water, between the composition's water and nanoparticles. Titanium oxide (TiO_2) nanoparticles, mixed and suspended in water to produce a nanofluid with specifications were used in practical testing to evaluate the solar collector (A). According to Refs.[21-23]. The following equation combines nanosolids with water.

$$m_p = \frac{\emptyset \times \rho_p \times \left(\frac{m_f}{\rho_f}\right)}{(1-\emptyset)} \quad (1)$$

The equation itself is a calculation for the mass of the mixture (m_p) based on the volume fraction of the solid phase ($\emptyset$), the density of the solid phase (ρ_p), the mass of the fluid phase (m_f), the density of the fluid phase (ρ_f), and the complement of the volume fraction of the solid phase ($1-\emptyset$). Table 2 describes the characteristics of the TiO_2.

Table 2 Nanoparticles' thermal and physical characteristics

Subject	Density (kg/m^3)	Specific heat (J/kg)	Thermal conductivity coefficient (W/mK)	Viscosity (kg/m·s)
Titanium oxide	3895	692	8.4	—

Using Eq. (1), a sensitive scale determined the number of nanoparticles needed to mix with water. Fig.2(d) shows this scale device, while Fig.2(e) shows the ultrasound nano equipment. Two ways combine solid nanoparticles with water after finding their quantity: We dissolved nanoparticles in water in two steps based on Refs.[24] and [25].

2.1 Second Procedure Entails the Use of an Ultrasound Device

For 40 min, an electric mixer combined nanoparticles and water until it was completely homogeneous. Using an ultrasonic tool to evenly distribute nanoparticles in the mixture. This procedure needs many steps. The test equipment fed nanofluid to the basin and continuously mixed it with an electric mixer to suspend and disperse nanoparticles[26]. Following the nanofluid till particle separation ensured water distribution. Water-titanium oxide nanofluid volumetric stability constant peaks at 12 h (0.5%). Nanofluid samples monitoring photo are described in Fig.4. The trials showed stability of TiO_2 in water.

Fig. 4 Titanium dioxide at the nanoscale (0.5% TiO_2-Water) being checked in action, photographed

2.2 Physical Interpretations and Discussion

Nanofluid density, thermal conductivity, viscosity, and specific heat were measured experimentally.

2.2.1 Density

The mathematical expression that relates to the density (ρ) written as Eq. (2):

$$\rho = \frac{m}{v} \tag{2}$$

where m is the mass, measured by a sensitive balance, and v is the water volume, measured by a graduated beaker.

2.2.2 Thermal conductivity

Heat conduction is thermal conductivity. Conductivity Meters (TS-51) assessed water and nanofluid thermal conductivity with 0.01% accuracy as shows in Fig. 2(f). Insert the cylindrical component into the water sample, then place the nanofluid sample in the center of the beaker at the desired temperature. We reread the samples three times.

2.2.3 Viscosity

The Brookfield Digital Viscometer DV-II+ Pro as shown in Fig. 2(g) measures nanofluid and water viscosities using torque (shear stress). Device precision is 0.01%. We added water and nanofluids. Rotating the device's bottom cylinder in the fluid's graded flask measures viscosity, as shown in Fig.2 (g).

2.3 Solar Collector Configuration and Mathematical Formulation

Two flat solar collectors of identical size, one using distilled water and the other using a nanofluid with 0.5% titanium oxide, were installed on the roof of a Kirkuk residential house building for practical testing. Nine temperature sensors and a memory card reader gather data. It stores discoveries in 16 GB. These methods were used to study mass flow rate and radiation intensity on a flat solar collector in Kirkuk's climate in March and April. To install the solar

collector, first, it is important to clean the compound's outside to remove any dust and dirt on the solar collector's glass. This will prevent the sun's energy from being weakened and skewing the data. Next, add water to the tank and distribute it via the pipe system using the relief valve. The grid-backed UPS and pipe water are connected through the system. A flow meter is used to measure water flow in the solar collector since mass flow was 0.02, 0.009, 0.009, 0.0045 kg/s. It is also important to check all sensor positions for accuracy before proceeding.

To ensure accurate readings, it is necessary to restart the Arduino before taking measurements. The measurements should be taken from 9∶00 to 17∶00 using the Arduino device to measure and record sun radiation for each hour of the test. Additionally, wind and ocean temperatures should be measured with meteorology. Record the mass flow (kg/s) for both collectors, which varies from 0.0045 to 0.02 during the hourly processes. Thermocouples, mass flux, and solar radiation intensity meters were used in studies to show their error percentage. The error rate was less than 1% for temperatures, 2% for mass flow, and 0.5% for solar radiation.

Calculation of the heat extraction coefficient (FR):

$$F_{\mathrm{R}} = \frac{\dot{m}\, c_{\mathrm{p}} F}{A_{\mathrm{c}}\, U_{\mathrm{L}}}\left(1 - e^{\frac{-A_{\mathrm{c}} U_{\mathrm{L}} F}{\dot{m} c_{\mathrm{pf}}}}\right) \tag{3}$$

This equation involves variables such as mass flow rate (m_{c}), specific heat capacity (c_{p}), cross-sectional area (A_{c}), overall heat transfer coefficient (U_{L}), and a coefficient (F). The useful heat gain (Q_{u}) is estimated from Eq. (4).

$$Q_u = A_{\mathrm{c}}\, F_{\mathrm{R}} [\tau\alpha\, I_{\mathrm{T}} - U_{\mathrm{L}}(T_{\mathrm{PM}} - T_{\mathrm{a}})] \tag{4}$$

The equation considers variables such as correction factor (τ), heat transfer coefficient (α), incident thermal radiation (I_{T}), overall heat transfer coefficient (U_{L}), mean temperature (T_{PM}), and ambient temperature (T_{a}). The thermal efficiency (η_c) is evaluated from Eq.(5).

$$\eta_{\mathrm{c}} = \frac{Q_{\mathrm{u}}}{A_{\mathrm{c}}\, I_{\mathrm{T}}} \tag{5}$$

To calculate thermos generated entropy, the Eq. (6) below is used:

$$\dot{S}_{\mathrm{gen,th}} = \dot{m}\, C_p \ln\left(\frac{T_{\mathrm{o}}}{T_{\mathrm{i}}}\right) - \left(\frac{\dot{Q}_{\mathrm{s}}}{T_{\mathrm{s}}}\right) + \left(\frac{\dot{Q}_{\mathrm{o}}}{T_{\mathrm{a}}}\right) \tag{6}$$

In Eq.(6), the first term, $\dot{m}\, C_p \ln\left(\frac{T_{\mathrm{o}}}{T_{\mathrm{i}}}\right)$ represents the rate of entropy generation due to heat transfer within the system. The second term, $(\dot{Q}_s / T_s)$ represents the rate of entropy generation due to heat transfer to the surroundings. The third term, $(\dot{Q}_{\mathrm{o}} / T_{\mathrm{a}})$ represents the rate of entropy generation due to heat transfer into the system from the surroundings. The Exergy Energy Efficiency (η_{ex}) or the second law efficiency of the solar collector is calculated from Eq. (7) below:

$$\eta_{\mathrm{ex}} = 1 - \frac{T_{\mathrm{a}}\, \dot{S}_{\mathrm{gen}}}{\left[1 - \left(\frac{T_{\mathrm{a}}}{T_{\mathrm{s}}}\right)\right] \dot{Q}_{\mathrm{s}}} \tag{7}$$

Thermally exergy destruction is calculated from Eq.(8) below:

$$\dot{E}\, x_{\mathrm{dest,th}} = T_{\mathrm{a}}\, \dot{S}_{\mathrm{gen,th}} \tag{8}$$

The flat solar collector's heat transfer coefficient, heat energy obtained, heat extraction coefficient, total heat loss coefficient, entropy generated, exergy created, and practical and theoretical efficiency were perfected. The experiment used two solar collector case studies. The first scenario employed water to find the flat solar collector's efficiency gain 0.0135%, 0.02%.

3 Thermophysical Characterization of Aqueous Nanofluid

Titania nanofluid's thermophysical properties were measured experimentally. Density, viscosity, and heat conductivity are thermodynamic properties. Fig. 5 shows that at 0.5% concentration, thermal conductivity is 10.2% higher than pure water at 30 ℃ and even higher at 60 ℃. Nanofluid thermal conductivity rises faster than pure water with temperature.

Between 9∶00 a. m. and 17∶00 p.m., time-lapse measurements of the nanofluid in the flat solar collector's temperature and mass flow rate were taken. This data was used to evaluate several critical parameters. Solar radiation peaks at 810 W/m^2 at midday in April and 805 W/m^2 in March before swiftly declining to its annual low towards the end of the year. In March, the time test is 695 W/m^2, and in April, 700 W/m^2. Fig. 6 illustrates that April 2022 will have the highest radiation intensity at noon in Kirkuk, Iraq.

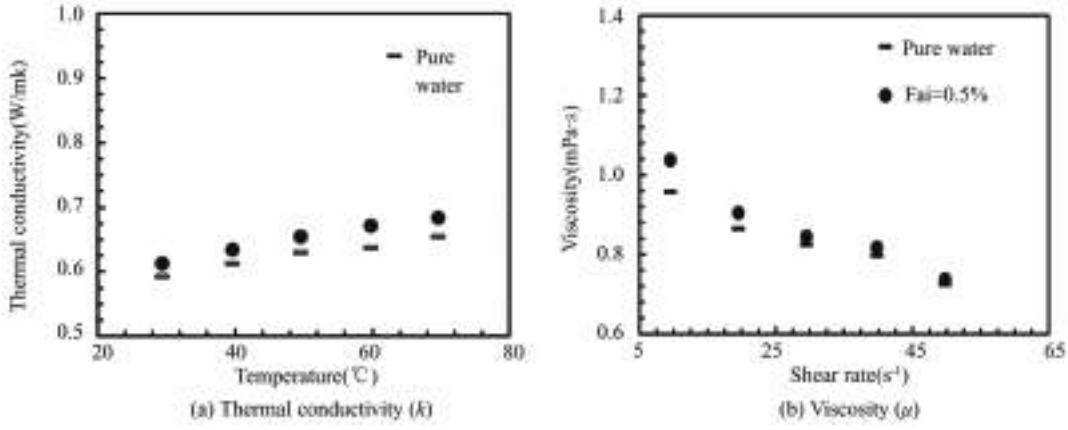

Fig.5 Thermal conductivity and viscosity

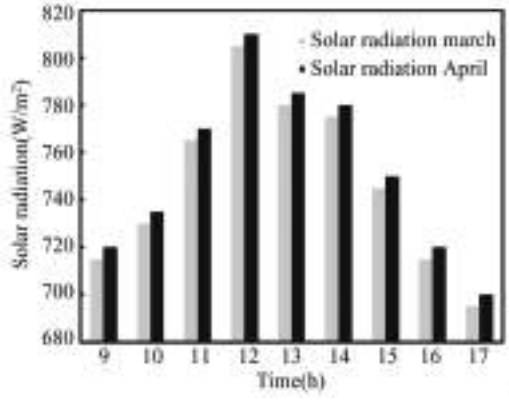

Fig.6 March and April average solar radiation intensity in Kirkuk, Iraq, in the year 2022

Due to solar radiation variation, water and titanium oxide collector efficiency climbed to 48% and 50% at noon in March with a mass flow rate of 0.02 kg/s. As proved in Fig.6, solar radiation finds its maximum value. Since energy is directly proportional to fluid mass flow rate, the solar collector's efficiency depends on solar radiation intensity. Titanium oxide nanofluids enhance collector performance due to their significant thermal expansion and improved natural convection, particularly at noon, the nanofluid titanium oxide is 21% higher than pure water. At noon in April at a mass flow rate of 0.2 kg/s, the instantaneous collector efficiency of water and titanium oxide reached 47.47% and 50.67%, respectively, as solar radiation peaked, as illustrated in Figs. 7 – 10. Nanofluids with 0.5% titanium oxide have a 6.3% higher temperature than pure water at noon when solar energy is at its greatest. The collector's efficiency decreases by 0.79% for pure water and 0.53% for titanium oxide at 17:00 in the evening at 0.2 kg/s.

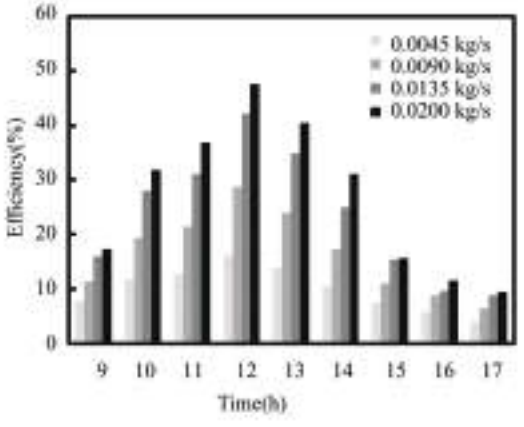

Fig.7 Efficiency vs mass flow rate for nanofluids with Pure water(The Kirkuk, Iraq, March 2022 test standard)

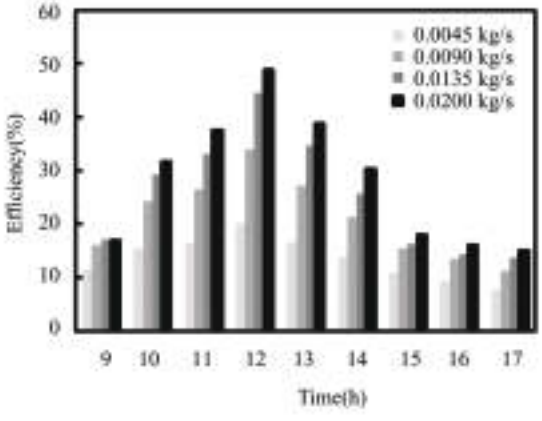

Fig.8 Efficiency vs mass flow rate for nanofluids with 0.5% TiO_2(The Kirkuk, Iraq, March 2022 test standard)

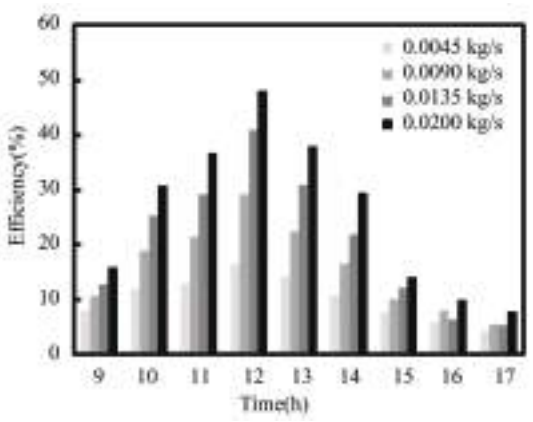

Fig.9 Efficiency vs mass flow rate for nanofluids with Pure water (The Kirkuk, Iraq, April 2022 test standard)

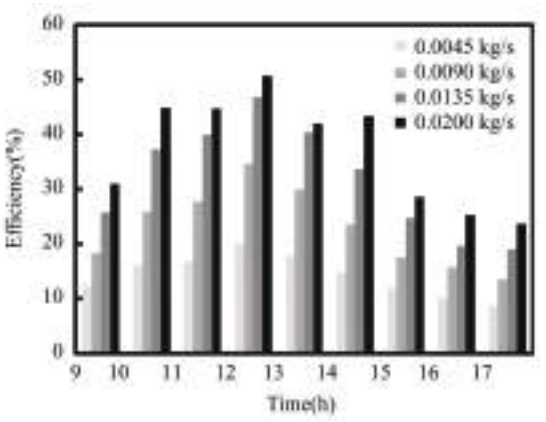

Fig.10 Efficiency vs mass flow rate for nanofluids with 05% TiO_2(The Kirkuk, Iraq, April 2022 test standard)

Figs.11 and 12 show that the amount of heat energy gained practically by pure water from the solar collector at various mass flow rates ranging from 0.0045 − 0.020 kg/s rises with sunrise until it reaches its maximum value at noon due to the increase in radiation falling on the solar collector, and then it gradually decreases for two months (March and April). April has more compound time than March. The highest usable energy is recorded in the forgotten month at 0.02 kg/s mass flow rate due to sun radiation variance. This is because solar energy density and fluid mass flow rate are related to useful energy. April's high air temperature reduced losses, increasing useful energy by 3.2% compared to March at the same mass flow rate. Figs.13 and 14 illustrate how much thermal energy a titanium oxide nanofluid at 0.5% of the solar collector gains at mass flow rates from 0.0045 kg/s to 0.020 kg/s. After rising consistently throughout the morning, the radiation hitting the solar collector peaks at midday and diminishes over the next two months (March and April). In April, radiation intensity fell on the complex was higher than in March, thus forgetfulness peaked at about 410 W at noon. Due to sun radiation variance, we record the highest figure in the forgetful month at 0.02 kg/s mass flow rate. This is because solar energy density and fluid mass flow rate are related to useful energy. Nanofluid titanium oxide increases useable energy by 0.5% in March and 0.6% in April compared to water.

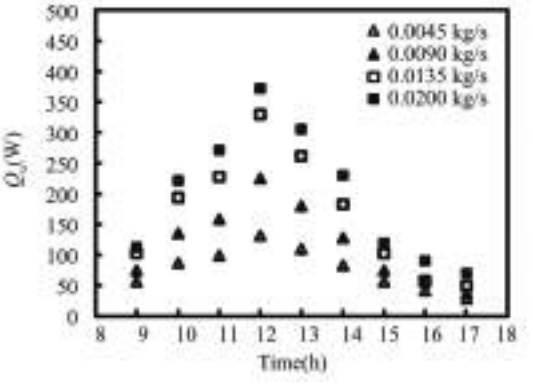

Fig.11 The energy gained from pure water in Kirkuk, Iraq, in March 2022 compared to daylight hours

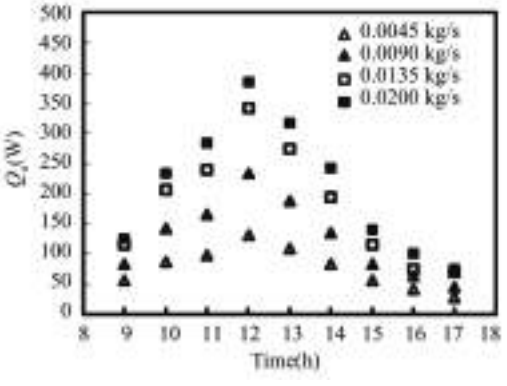

Fig.12 The energy gained from pure water in Kirkuk, Iraq, in April 2022 compared to daylight hours

3.1 Thermal Entropy Generation

Thermal entropy is produced by thermodynamic processes. It is caused by heat transmission, fluid friction, and mixing. Thermal entropy, which is produced by all physical processes, severely restricts energy conversion. Thermal entropy generation is used by engineers and scientists to optimize power plants, refrigeration cycles, and heat exchangers. Reducing thermal entropy generation boosts efficiency while lowering environmental impact. The thermos generated

entropy of the current method quantifies the performance degradation of the flat solar collector. The graphs depict the thermogenerated entropy-Reynolds number relationship over the course of two months, as illustrated in Figs.15 and 16. When the Reynolds numbers of pure water and titanium oxide nanofluid increase by 0.5%, thermal entropy falls. Pure water and titanium oxide had the highest levels of thermally generated entropy at 9:00 a.m. in March and April, with values of 2.98 and 2.97 W/k, respectively. According to these findings, water has the highest value of produced entropy. Because the physical properties of nanofluids vary with volumetric concentration, the entropy value rises and reaches a minimum at midday, and the Reynolds number has a specific value for nanofluids. When solar radiation falls, thermal entropy rises. Collector efficiency and entropy generation aid in the evaluation of nanofluid-based FPCs.

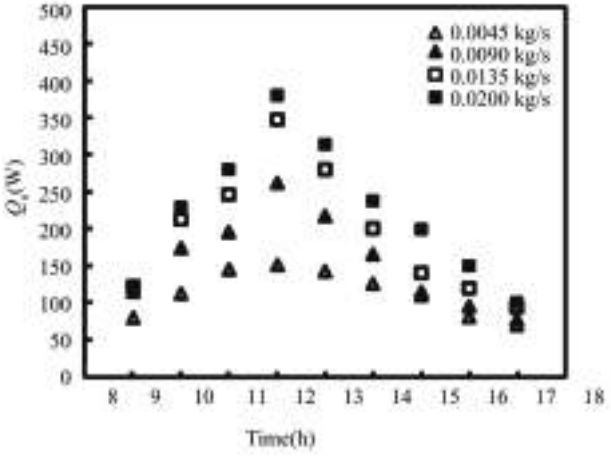

Fig.13 Gain in energy produced by employing 0.5% titanium oxide in March 2022 in Kirkuk, Iraq

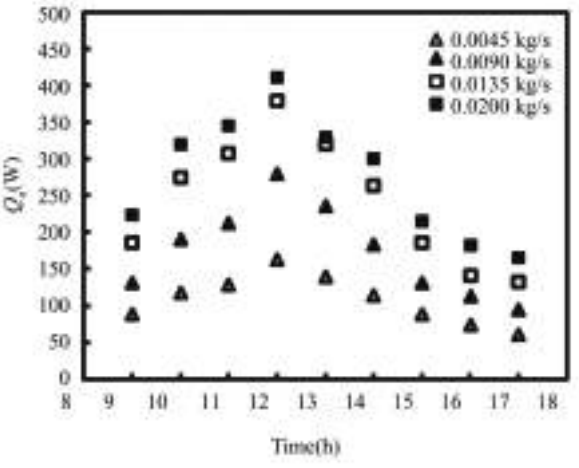

Fig.14 Gain in energy produced by employing 0.5% titanium oxide in April 2022 in Kirkuk, Iraq

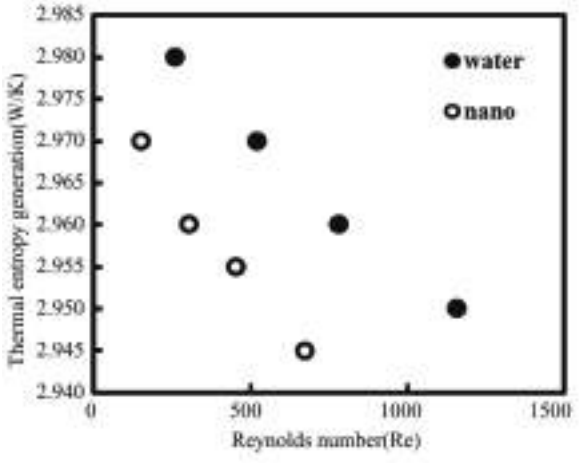

Fig.15 The thermal entropy of both pure water and nanofluid rose by 0.5% in March 2022 in Kirkuk, Iraq

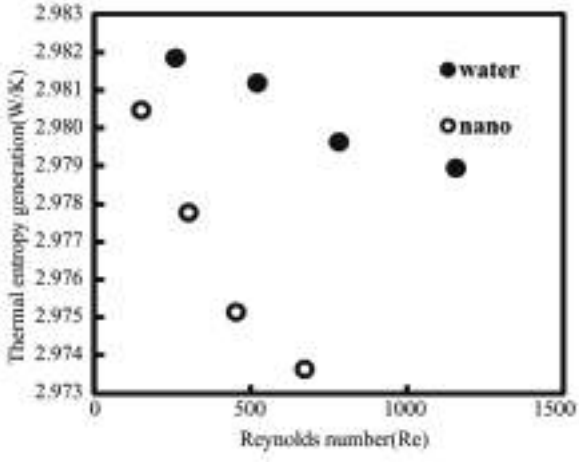

Fig.16 The thermal entropy of both pure water and nanofluid rose by 0.5% in April 2022 in Kirkuk, Iraq

Flat solar collectors' exergy efficiency increases with sunlight in March, until reaches 0.0045 kg/s, as described in Figs.17 and 18. The flat solar collector's efficiency drops as solar radiation intensity diminishes after midday in March and April. Nanofluids improve the physical parameters of the fluid used throughout the test, increasing the exergy efficiency of the flat solar collector by 0.4%, 0.3%, 0.2%, and 0.08% for flow masses of 0.02, 0.0135, 0.09, and 0.0045 kg/s. Figs.19 and 20 show how increasing solar radiation in a flat solar collector boosts exergy efficiency in April. The flat solar collector's mass flux, 0.0045 kg/s during midday, directly affects its efficiency. After midday, solar radiation intensity decreases, lowering mass flux. Water with 0.5% titanium oxide nanoparticles at the flow rates of 0.02, 0.0135, 0.009, and 0.0045 kg/s boosts exergy efficiency.

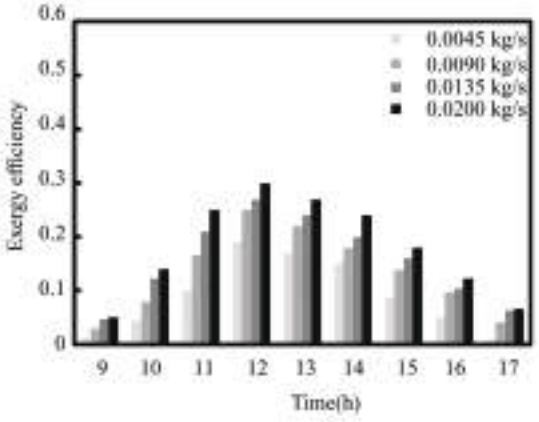

Fig.17 Exergy efficiency over time in March of 2022 in Kirkuk, Iraq, at varied flows of pure water

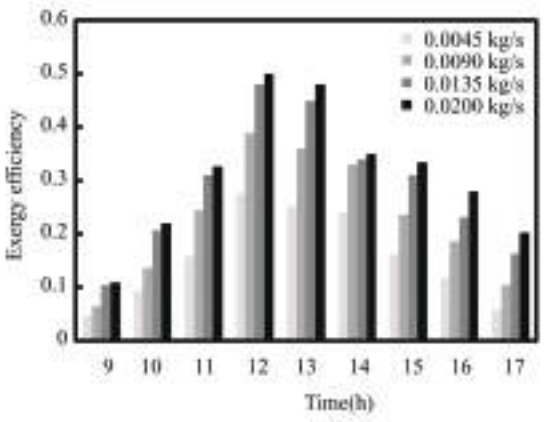

Fig.18 Exergy efficiency for nanofluid titanium oxide at 0.5% flow rate in March 2022 in Kirkuk, Iraq

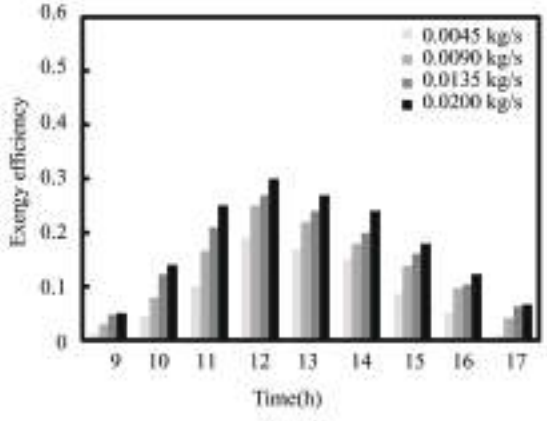

Fig.19 Exergy efficiency over time in April of 2022 in Kirkuk, Iraq, at varied flows of pure water

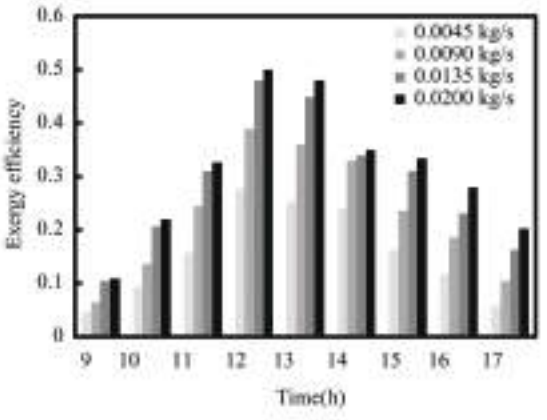

Fig.20 Exergy efficiency for nanofluid titanium oxide at 0.5% flow rate in April 2022 in Kirkuk, Iraq

3.2 Comparison of Exergy Efficiency with Thermal Efficiency

This study evaluates flat solar collector efficiency and performance. Maximize thermo-exergy efficiency. Exergy efficiency measures solar light-to-thermal energy conversion. Heat transfer, fluid dynamics, and system structure affect power utilization. A nanofluid improved the flat solar collector's physical characteristics and thermal losses, enhancing exergy efficiency. Researchers studied the solar collector's efficiency (practically and theoretically), entropy production, exergy creation, heat transfer coefficient, heat energy acquisition, heat extraction coefficient, total heat loss coefficient, and heat transfer coefficient. Titanium oxide nanoparticles in flat solar collector water increased thermal and exergy efficiency as the study revealed. Nanoparticles improved energy gain and process losses, increasing exergy efficiency. Figs. 21 and 22 show Kirkuk's thermal and exergy efficiency at 0.02 kg/s for pure water and nanofluid titanium oxide. Solar radiation peaks between 9 a.m. and 12 p.m., and energy and thermal efficiency diminish between 12 p. m. and 5 p.m. Pure water and nanofluid have better heat transmission, energy acquisition, and entry-exit temperature differential. As the day progresses and the temperature rises, thermal losses in the flat solar collector diminish, boosting clean water and nanofluid thermal and exergy efficiency.

3.3 Exergy Destruction Changes Throughout Time

Operating conditions, input/output quality, and equipment age effect exergy destruction. Older equipment wastes energy. Pressure and temperature destroy system exergy. Fuel and waste quality affect exergy destruction efficiency. Monitoring exergy decay may show trends or outliers that affect system performance and longevity. The flat solar collector that circulated clean water and nanofluids lost energy in March and April, as illustrated in Figs. 23 – 26.

March and April have the weakest sun, peaking around midday and reversing direction after lunch. Breaking uses 0.02 kg/s. Thermal energy is strongest and broken thermal energy is lowest during midday solar radiation and ambient temperature. Heat from 0.5% titanium oxide particles in a nanofluid lowers crushing energy.

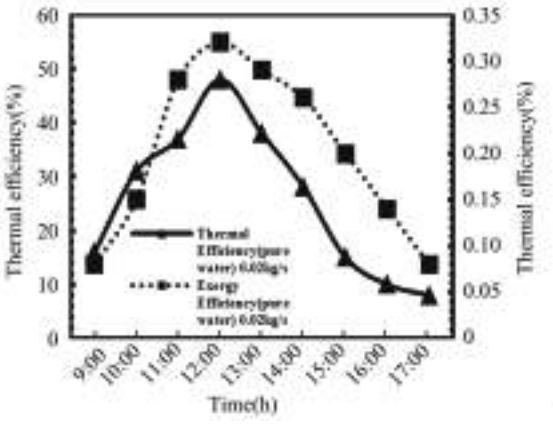

Fig.21 Thermal and exergy efficiency for March 2022 Kirkuk, Iraq, at 0.02 kg/s

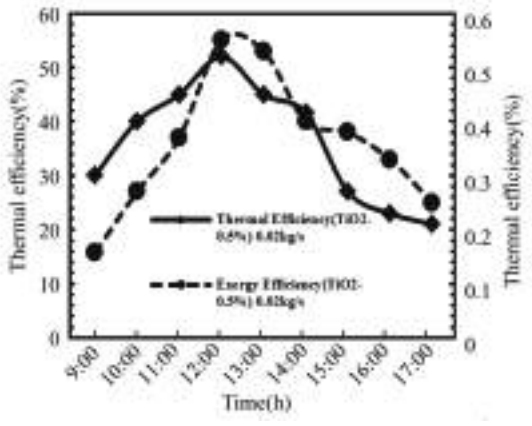

Fig.22 Thermal and exergy efficiency for April 2022 Kirkuk, Iraq, at 0.02 kg/s

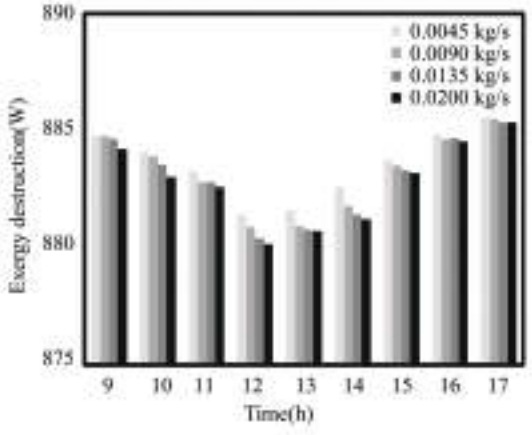

Fig.23 Exergy destruction in March 2022, Kirkuk, Iraq, with changing pure water flow rates

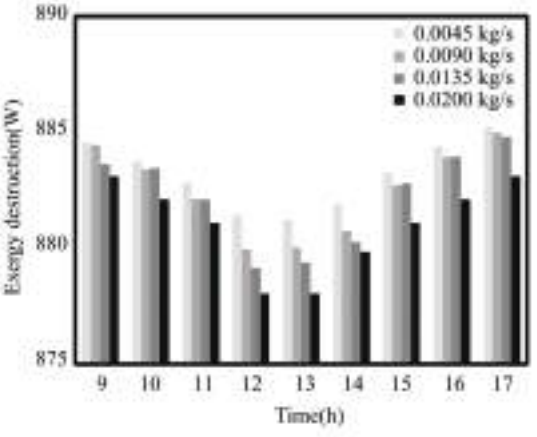

Fig.24 Exergy destruction with time for March & varied flow rates for TiO_2 nanofluid 0.5% in 2022 Kirkuk, Iraq

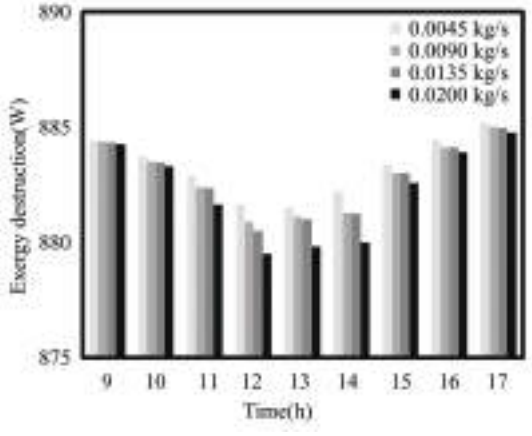

Fig.25 Exergy destruction in April 2022, Kirkuk, Iraq, with changing pure water flow rates

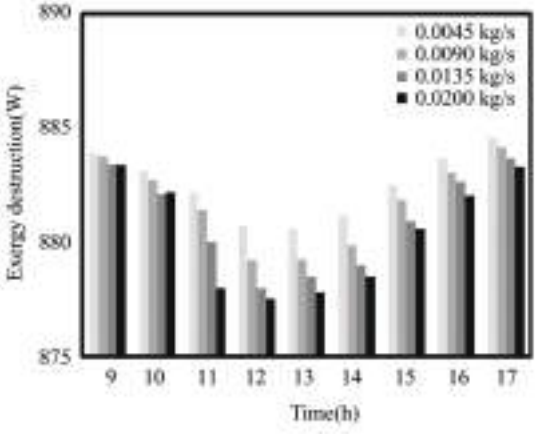

Fig.26 Exergy destruction with time for April & varied flow rates for TiO_2 nanofluid 0.5% in 2022 Kirkuk, Iraq

4 Conclusions

The experiment showed that nanofluid titanium oxide can increase the efficiency of flat solar collectors in terms of heat energy gain and exergy efficiency. At noon in March and April, with a mass flow rate of 0.02 kg/s, water and titanium oxide collector efficiency climbed to 48% and 50%, respectively, due to the relationship between solar energy density and fluid mass flow rate. The use of nanofluid titanium oxide increased usable energy by 0.5% in March and 0.6% in April compared to water. The thermal entropy generated by all physical processes restricts energy conversion, and reducing thermal entropy generation can boost efficiency while lowering environmental impact. The experiment showed that the flat solar collector's exergy efficiency increases with sunlight in March until it reaches 0.0045 kg/s, and the efficiency drops as solar radiation intensity diminishes after midday in March and April.

References

[1] Yousefi T, Veisy F, Shojaeizadeh E, et al. An experimental investigation on the effect of MWCNT-H_2O nanofluid on the efficiency of flat-plate solar collectors. Experimental Thermal and Fluid Science, 2012, 39: 207-212. DOI: 10.1016/j.expthermflusci.2012.01.025.

[2] Vijayakumaar S C, Lakshmi Shankar R, Babu K. Effect of CNT-H_2O nanofluid on the performance of solar flat plate collector-an experimental investigation. Proceedings of the International Conference on Advanced Nanomaterials & Emerging Engineering Technologies. Chennai.2013.197-199. DOI: 10.1109/ICANMEET.2013.6609275.

[3] Zamzamian A, KeyanpourRad M, KianiNeyestani M, et al. An experimental study on the effect of Cu-synthesized/EG nanofluid on the efficiency of flat-plate solar collectors. Renewable Energy, 2014, 71: 658-664. DOI: 10.1016/j.renene.2014.06.003.

[4] Nasrin R, Alim M A. Semi-empirical relation for forced convective analysis through a solar collector. Solar Energy, 2014, 105: 455-467. DOI: 10.1016/j.solener.2014.03.035.

[5] Moghadam A J, Farzane-Gord M, Sajadi M, et al. Effects of CuO/water nanofluid on the efficiency of a flat-plate solar collector. Experimental Thermal and Fluid Science, 2014, 58: 9-14. DOI: 10.1016/j.expthermflusci.2014.06.014.

[6] Michael J J, Iniyan S. Performance of copper oxide/water nanofluid in a flat plate solar water heater under natural and forced circulations. Energy Conversion and Management, 2015, 95: 160-169. DOI: 10.1016/j.enconman.2015.02.017.

[7] Said Z, Sabiha M A, Saidur R, et al. Performance enhancement of a Flat Plate Solar collector using Titanium dioxide nanofluid and Polyethylene Glycol dispersant. Journal of Cleaner Production, 2015, 92: 343-353. DOI: 10.1016/j.jclepro.2015.01.007.

[8] Salavati Meibodi S, Kianifar A, Niazmand H, et al. Performance enhancement of a flat plate solar collector using titanium dioxide nanofluid and Polyethylene Glycol dispersant. Internation Communcation in Heat and Mass Transfer, 2015, 65: 71-75. DOI: 10.1016/j.icheatmasstransfer.2015.02.011.

[9] Vakili M, Hosseinalipour S M, Delfani S, et al. Experimental investigation of graphene nanoplatelets nanofluid-based volumetric solar collector for domestic hot water systems. Solar Energy, 2016, 131: 119-130. DOI: 10.1016/j.solener.2016.02.034.

[10] Verma S K, Tiwari A K, Chauhan D S. Performance augmentation in flat plate solar collector using MgO/water nanofluid. Energy Conversion and Management, 2016, 124: 607-617. DOI: 10.1016/j.enconman.2016.07.007.

[11] Jouybari H J, Saedodin S, Zamzamian A, et al. Effects of porous material and nanoparticles on the thermal performance of a flat plate solar collector: An experimental study. Renewable Energy, 2017, 114: 1407-1418. DOI: 10.1016/j.renene.2017.07.008.

[12] Syam Sundar L, Singh M K, Punnaiah V, et al. Experimental investigation of Al_2O_3/water nanofluids on the effectiveness of solar flat-plate collectors with and without twisted tape inserts. Renewable Energy, 2018, 119: 820-833. DOI: 10.1016/j.renene.2017.10.056.

[13] Zarda F, Hussein A M, Danook S H, et al. Enhancement of thermal efficiency of nanofluid flows in a flat solar collector using CFD. 2022, 23(4): 1-9. DOI: 10.29354/diag/156384.

[14] Kiliç F, Menlik T, Sözen A. Effect of titanium dioxide/water nanofluid use on thermal performance of the flat plate solar collector. Solar Energy, 2018, 164: 101-108. DOI: 10.1016/j.solener.2018.02.002.

[15] Sharafeldin M A, Gróf G. Experimental investigation of flat plate solar collector using CeO_2-water nanofluid. Energy Conversion and Management, 2018, 155: 32-41. DOI: 10.1016/j.enconman.2017.10.070.

[16] Tong Y, Lee H, Kang W, et al. Energy and exergy comparison of a flat-plate solar collector using water, Al_2O_3 nanofluid, and CuO nanofluid. Applied Thermal Engineering, 2019, 159: 113959. DOI: 10.1016/j.applthermaleng.2019.113959.

[17] Nirmala P N. Comparative studies on efficiency of single and double glassed solar water heater. Materials Today: Proceedings, 2021, 34(Part 2): 420-424. DOI: 10.

1016/j.matpr.2020.02.204.

[18] Choudhary S, Sachdeva A, Kumar P. Influence of stable zinc oxide nanofluid on thermal characteristics of flat plate solar collector. Renewable Energy, 2020, 152: 1160 - 1170.DOI: 10.1016/j.renene.2020.01.142.

[19] Okonkwo E C, Wole-Osho I, Kavaz D, et al. Thermodynamic evaluation and optimization of a flat plate collector operating with alumina and iron mono and hybrid nanofluids. Sustainable Energy Technologies and Assessments, 2020, 37: 100636. DOI: 10. 1016/j. seta. 2020.100636.

[20] Alklaibi A M, Sundar L S, Sousa A C M. Experimental analysis of exergy efficiency and entropy generation of diamond/water nanofluids flow in a thermosyphon flat plate solar collector. International Communication in Heat and Mass Transfer, 2021, 120: 105057. DOI: 10. 1016/j. icheatmasstransfer.2020.105057.

[21] Javadi F S, Sadeghiporu S, Saidur R, et al. The effects of nanofluid on thermophysical properties and heat transfer characteristics of a plate heat exchanger. International Communications in Heat and Mass Transfer, 2013, 44: 58 - 63. DOI: 10. 1016/j. icheatmasstransfer. 2013.0.

[22] Ramachandran K, Hussein A M, Kadirgama K, et al. Thermophysical properties measurement of nano cellulose in ethylene glycol/water. Applied Thermal Engineering, 2017, 123: 1158 - 1165. DOI: 10. 1016/j. applthermaleng. 2017.05.

[23] Ghorbani B, Akhavan-Behabadi M A, Ebrahimi S, et al. Experimental investigation of condensation heat transfer of R600a/POE/CuO nano-refrigerant in flattened tubes. International Communications in Heat and Mass Transfer, 2017, 88: 236 - 244. DOI: 10. 1016/j. icheatmasstransfer. 2017.0.

[24] Baby S, Johnson J. Numerical investigation on the heat transfer characteristics of alumina-water nanofluid in a double pipe heat exchanger. International Research Journal of Engineering and Technology (IRJET), 2018, 5(3): 3976-3983.

[25] Hussein A M, Khaleell O S, Danook S H. Enhancement of double-pipe heat exchanger effectiveness by using water - CuO. NTU Journal of Engineering and Technololgy, 2022, 1(2): 18-22. DOI: 10.56286/ntujet. v1i2.59.

[26] Singh R N, Rajat P, Lav I, et al. Experimental studies of nanofluid TiO_2/CuO in a heat exchanger (Double Pipe). Indian Journal of Science and Technology, 2016, 9(31): 1-6. DOI: 10.17485/ijst/2016/v9i31/93623.